Electronic Supplementary Material (ESI) for CrystEngComm.


## ELECTRONIC SUPPORTING INFORMATION

# On the pairwise cocrystallization of racemic compounds

**Fuli Zhou , Carole Body, Koen Robeyns, Tom Leyssens and Oleksii Shemchuk***

Institute of Condensed Matter and Nanosciences, Université catholique de Louvain, 1 Place Louis Pasteur, B-1348 Louvain-La-Neuve, Belgium.

Correspondence: oleksii.shemchuk@uclouvain.be

# Contents

## Chemical structure of the investigated compounds

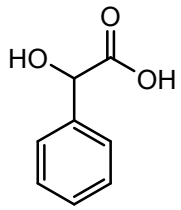

**Mandelic acid (MA)**

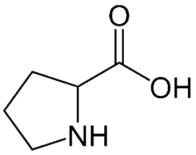

**Proline (PRO)**

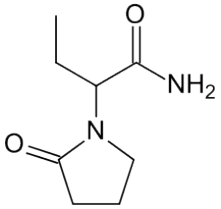

**Etiracetam (ETI)**

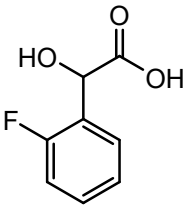

**2-Fluoromandelic acid (2-FMA)**

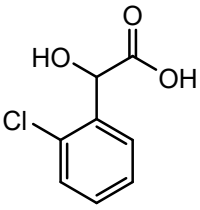

**2-Chloromandelic acid (2-ClMA)**

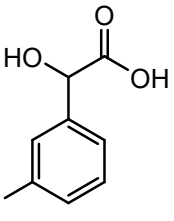

**3-Chloromandelic acid (3-ClMA)**

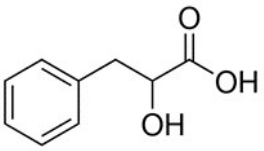

**3-phenyllactic acid (3-PLA)**

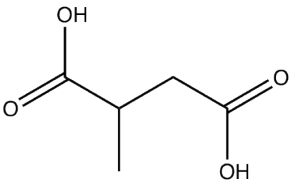

**Methylsuccinic acid (MSA)**

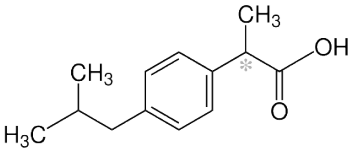

**Ibuprofen (IBU)**

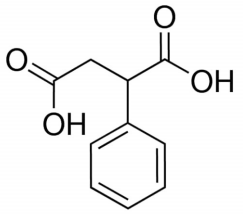

**Phenylsuccinic acid (PSA)**

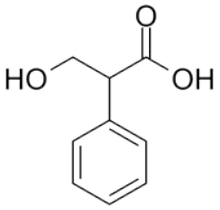

**Tropic acid (TRA)**

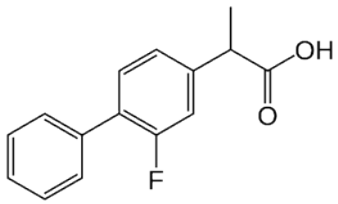

**Flurbiprofen (FLU))**

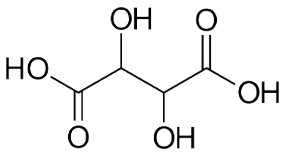

**Tartaric acid (TAR)**

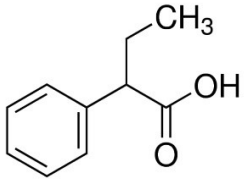

**2-Phenylbutyric acid (2-PBA)**

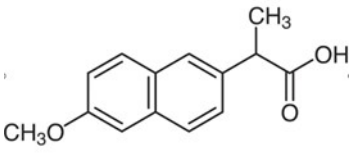

**Naproxen (NAP)**

**Scheme 1**. Chemical structures of the investigated compounds.

# Crystallographic data

**Table ESI-1**. Crystal data and structure refinement for the cocrystals with etiracetam.

| **Identification code** | **2-FMA·ETI** | **2-ClMA·ETI** | **3-ClMA·ETI** | **$(FLU)_2$·ETI** |
|---|---|---|---|---|
| **Empirical formula** | $C_{16}H_{21}FN_2O_5$ | $C_{16}H_{21}ClN_2O_5$ | $C_{16}H_{21}ClN_2O_5$ | $C_{38}H_{40}F_2N_2O_6$ |
| **Formula weight / g·mol$^{-1}$** | 340.35 | 356.80 | 356.80 | 658.72 |
| **Temperature / K** | 297(2) | 297(2) | 297(2) | 297(2) |
| **Crystal system** | Monoclinic | Monoclinic | Triclinic | Monoclinic |
| **Space group** | $P2_1$ | $P2_1$ | $P$-1 | $P2_1/c$ |
| **a / Å** | 11.8613(14) | 11.8318(7) | 7.7370(14) | 5.9135(3) |
| **b / Å** | 5.7602(7) | 5.8252(3) | 10.7279(12) | 18.5470(9) |
| **c / Å** | 13.2858(14) | 13.9008(8) | 11.583(2) | 31.3947(16) |
| **α / °** | 90 | 90 | 63.137(16) | 90 |
| **β / °** | 110.458(12) | 113.879(7) | 86.083(15) | 94.307(5) |
| **γ / °** | 90 | 90 | 84.134(13) | 90 |
| **Volume / Å$^3$** | 850.48(18) | 876.06(9) | 852.9(3) | 3433.6(3) |
| **Z** | 2 | 2 | 2 | 4 |
| **Density (calculated) / Mg·m$^{-3}$** | 1.329 | 1.353 | 1.389 | 1.274 |
| **Absorption coefficient / mm$^{-1}$** | 0.106 | 0.246 | 0.253 | 0.093 |
| **F(000)** | 360 | 376 | 376 | 1392 |
| **Crystal size / mm$^3$** | 0.50x 0.03 x 0.01 | 0.5 x 0.07 x 0.02 | 0.40 x 0.30 x 0.25 | 0.30x 0.02 x 0.01 |
| **θ range for data collection / °** | 3.143 to 25.230 | 2.925 to 25.685 | 3.262 to 26.147 | 2.825 to 20.821 |
| **Reflections collected** | 11056 | 11897 | 11062 | 12226 |
| **Independent reflections** | 3062 [R(int) = 0.0912] | 3314 [R(int) = 0.0451] | 3378 [R(int) = 0.0195] | 3561 [R(int) = 0.0571] |
| **Completeness %** | 99.7 to θ=25.231° | 99.8 to θ=25.242° | 99.1 to θ=25.242° | 99.3 to θ=20.821° |
| **Data / restraints / parameters** | 3062 / 1 / 220 | 3314 / 1 / 219 | 3378 / 5 / 232 | 3561 / 0 / 436 |
| **Goodness-of-fit on F$^2$** | 1.077 | 1.068 | 1.048 | 1.143 |
| **Final R indices [I>2sigma(I)]** | R1 = 0.0642, wR2 = 0.1171 | R1 = 0.0581, wR2 = 0.1563 | R1 = 0.0405, wR2 = 0.1019 | R1 = 0.0707, wR2 = 0.1271 |
| **R indices (all data)** | R1 = 0.1045, wR2 = 0.1298 | R1 = 0.0659, wR2 = 0.1620 | R1 = 0.0438, wR2 = 0.1045 | R1 = 0.1154, wR2 = 0.1414 |
| **Flack parameter** | -0.2(10) | 0.02(4) | | |

**Table ESI-2a**. Crystal data and structure refinement for the cocrystals with proline.

| **Identification code** | **2-PBA·PRO** | **3-PLA·PRO** | **IBU·PRO** | **MSA·PRO** | **PSA·PRO** |
|---|---|---|---|---|---|
| **Empirical formula** | $C_{15}H_{21}NO_4$ | $C_{14}H_{19}NO_5$ | $C_{18}H_{27}NO_4$ | $C_{10}H_{17}NO_6$ | $C_{30}H_{38}N_2O_{12}$ |
| **Formula weight / g·mol$^{-1}$** | 279.33 | 281.30 | 321.40 | 247.24 | 618.62 |
| **Temperature / K** | 297(2) | 297(2) | 297(2) | 297(2) | 297(2) |
| **Crystal system** | Orthorhombic | Orthorhombic | Monoclinic | Orthorhombic | Monoclinic |
| **Space group** | *Pca2$_1$* | *Pbca* | *P2$_1$/c* | *Pbca* | *Cc* |
| **a / Å** | 10.1357(7) | 10.4273(3) | 9.4241(7) | 9.8806(18) | 5.7579(8) |
| **b / Å** | 17.1919(16) | 9.0611(3) | 37.399(2) | 9.6156(19) | 19.399(3) |
| **c / Å** | 9.1265(7) | 30.1865(10) | 10.4169(11) | 25.364(6) | 27.176(3) |
| **α / °** | 90 | 90 | 90 | 90 | 90 |
| **β / °** | 90 | 90 | 90.501(8) | 90 | 90.640(12) |
| **γ / °** | 90 | 90 | 90 | 90 | 90 |
| **Volume / Å$^3$** | 1590.3(2) | 2852.10(16) | 3671.3(5) | 2409.8(8) | 3035.3(7) |
| **Z** | 4 | 8 | 8 | 8 | 4 |
| **Density (calculated) / Mg·m$^{-3}$** | 1.167 | 1.310 | 1.163 | 1.363 | 1.354 |
| **Absorption coefficient / mm$^{-1}$** | 0.084 | 0.100 | 0.081 | 0.113 | 0.105 |
| **F(000)** | 600 | 1200 | 1392 | 1056 | 1312 |
| **Crystal size / mm$^3$** | 0.20x 0.03 x 0.01 | 0.20 x 0.14 x 0.03 | 0.11x 0.03 x 0.01 | 0.10x 0.03 x 0.01 | 0.20x 0.03 x 0.01 |
| **θ range for data collection / °** | 3.107 to 21.958 | 3.054 to 25.235 | 2.928 to 22.439 | 2.613 to 20.944 | 2.998 to 18.939 |
| **Reflections collected** | 6801 | 17328 | 15139 | 7426 | 2332 |
| **Independent reflections** | 1906 [R(int) = 0.0660] | 2572 [R(int) = 0.0483] | 4669 [R(int) = 0.0788] | 1270 [R(int) = 0.1096] | 2332 [R(int) = /]† |
| **Completeness %** | 98.4 to θ = 21.958° | 99.6 to θ = 25.235° | 98.2 to θ = 22.439° | 99.3 to θ = 20.944° | 98.1 to θ = 18.939° |
| **Data / restraints / parameters** | 1906 / 148 / 241 | 2572 / 33 / 212 | 4669 / 350 / 591 | 1270 / 0 / 157 | 2332 / 366 / 398 |
| **Goodness-of-fit on F$^2$** | 1.053 | 1.038 | 1.065 | 1.151 | 1.099 |
| **Final R indices [I>2sigma(I)]** | R1 = 0.0567, wR2 = 0.1433 | R1 = 0.0531, wR2 = 0.1350 | R1 = 0.0611, wR2 = 0.1410 | R1 = 0.0819, wR2 = 0.1632 | R1 = 0.0819, wR2 = 0.1907 |
| **R indices (all data)** | R1 = 0.0779, wR2 = 0.1544 | R1 = 0.0714, wR2 = 0.1453 | R1 = 0.0994, wR2 = 0.1631 | R1 = 0.1073, wR2 = 0.1773 | R1 = 0.1125, wR2 = 0.2203 |
| **Flack** | -1.3(10)* | | | | -1.3(10)* |

†Twinned data, refined against HKLF5 formatted data, imposing Merg 0.
*polar space group

**Table ESI-2b**. Crystal data and structure refinement for the cocrystals with proline.

| **Identification code** | **TSA·PRO** | **3-ClMA·PRO** | **2-FMA·PRO form I** | **2-FMA·PRO form II** | **MA·PRO** |
|---|---|---|---|---|---|
| **Empirical formula** | $C_{14}H_{19}NO_5$ | $C_{13}H_{16}ClNO_5$ | $C_{13}H_{16}FNO_5$ | $C_{13}H_{16}FNO_5$ | $C_{13}H_{17}NO_5$ |
| **Formula weight / g·mol$^{-1}$** | 281.30 | 301.72 | 285.27 | 285.27 | 267.27 |
| **Temperature / K** | 297(2) | 297(2) | 297(2) | 297(2) | 293(2) |
| **Crystal system** | Monoclinic | Triclinic | Triclinic | Monoclinic | Triclinic |
| **Space group** | *$P2_1/n$* | *P-1* | *P-1* | *$P2_1/c$* | *P-1* |
| **a / Å** | 11.2568(8) | 7.0457(14) | 7.406(5) | 12.591(2) | 7.0962(13) |
| **b / Å** | 5.7371(3) | 8.2146(9) | 8.459(2) | 8.7414(12) | 8.306(2) |
| **c / Å** | 22.5561(18) | 13.342(3) | 12.281(7) | 12.6758(14) | 12.120(3) |
| **α / °** | 90 | 106.407(14) | 102.89(4) | 90 | 103.74(2) |
| **β / °** | 103.029(8) | 90.268(16) | 101.66(6) | 104.824(14) | 99.820(18) |
| **γ / °** | 90 | 106.101(14) | 103.44(4) | 90 | 105.63(2) |
| **Volume / Å$^3$** | 1419.21(18) | 708.8(2) | 702.8(7) | 1348.7(4) | 646.9(3) |
| **Z** | 4 | 2 | 2 | 4 | 2 |
| **Density (calculated) / Mg·m$^{-3}$** | 1.317 | 1.414 | 1.348 | 1.405 | 1.372 |
| **Absorption coefficient / mm$^{-1}$** | 0.100 | 0.288 | 0.112 | 0.117 | 0.106 |
| **F(000)** | 600 | 316 | 300 | 600 | 284 |
| **Crystal size / mm$^3$** | 0.14x 0.06 x 0.02 | 0.20 x 0.15 x 0.02 | 0.05x 0.02 x 0.01 | 0.22x 0.15 x 0.08 | 0.40 x 0.15 x 0.10 |
| **θ range for data collection / °** | 3.670 to 23.262 | 3.022 to 25.237 | 2.993 to 18.845 | 3.094 to 25.260 | 2.668 to 26.212 |
| **Reflections collected** | 6149 | 9168 | 2190 | 8414 | 8814 |
| **Independent reflections** | 2030 [R(int) = 0.0473] | 2557 [R(int) = 0.0457] | 1057 [R(int) = 0.1060] | 2434 [R(int) = 0.0333] | 2534 [R(int) = 0.0546] |
| **Completeness %** | 99.2 to θ = 23.262° | 99.6 to θ = 25.237° | 96.1 to θ = 18.845° | 99.5 to θ = 25.242° | 98.0 to θ = 25.242° |
| **Data / restraints / parameters** | 2030 / 27 / 218 | 2557 / 143 / 253 | 1057 / 0 / 181 | 2434 / 0 / 184 | 2534 / 60 / 195 |
| **Goodness-of-fit on F$^2$** | 1.096 | 1.059 | 1.002 | 1.131 | 1.068 |
| **Final R indices [I>2sigma(I)]** | R1 = 0.0809, wR2 = 0.1781 | R1 = 0.0577, wR2 = 0.1343 | R1 = 0.0706, wR2 = 0.1209 | R1 = 0.0526, wR2 = 0.1190 | R1 = 0.0590, wR2 = 0.1638 |
| **R indices (all data)** | R1 = 0.1258, wR2 = 0.1990 | R1 = 0.0782, wR2 = 0.1441 | R1 = 0.1647, wR2 = 0.1526 | R1 = 0.0700, wR2 = 0.1267 | R1 = 0.0715, wR2 = 0.1740 |

**Table ESI-3**. Crystal data and structure refinement for the obtained polymorphs of the investigated structures.

| **Identification code** | **3-ClMA** | **PRO·$H_2O$** | **D-/L-3-phenyllactic acid** |
|---|---|---|---|
| **Empirical formula** | $C_8H_7ClO_3$ | $C_5H_{11}NO_3$ | $C_9H_{10}O_3$ |
| **Formula weight / g·mol$^{-1}$** | 186.59 | 133.15 | 166.17 |
| **Temperature / K** | 297(2) | 297(2) | 297(2) |
| **Crystal system** | Monoclinic | Monoclinic | Monoclinic |
| **Space group** | *$P2_1/c$* | *$P2_1/c$* | *$P2_1$* |
| **a / Å** | 16.6605(13) | 10.468(4) | 8.4198(11) |
| **b / Å** | 9.1572(5) | 5.3181(19) | 5.8428(7) |
| **c / Å** | 11.4407(8) | 12.162(5) | 8.6049(9) |
| **α / °** | 90 | 90 | 90 |
| **β / °** | 109.810(8) | 104.68(4) | 91.920(11) |
| **γ / °** | 90 | 90 | 90 |
| **Volume / Å$^3$** | 1642.1(2) | 655.0(5) | 423.08(9) |
| **Z** | 8 | 4 | 2 |
| **Density (calculated) / Mg·m$^{-3}$** | 1.509 | 1.350 | 1.304 |
| **Absorption coefficient / mm$^{-1}$** | 0.425 | 0.111 | 0.098 |
| **F(000)** | 768 | 288 | 176 |
| **Crystal size / mm$^3$** | 0.30x 0.20 x 0.15 | 0.25 x 0.15 x 0.10 | 0.20 x 0.16 x 0.15 |
| **θ range for data collection / °** | 2.924 to 25.254 | 3.463 to 22.439 | 3.330 to 26.278 |
| **Reflections collected** | 9586 | 3271 | 8426 |
| **Independent reflections** | 2932 [R(int) = 0.0513] | 828 [R(int) = 0.1008] | 1673 [R(int) = 0.0402] |
| **Completeness %** | 99.1 to θ = 25.242° | 97.3 to θ = 22.439° | 98.2 to θ = 25.242° |
| **Data / restraints / parameters** | 2932 / 154 / 247 | 828 / 60 / 113 | 1673 / 1 / 114 |
| **Goodness-of-fit on F$^2$** | 1.062 | 1.053 | 1.082 |
| **Final R indices [I>2sigma(I)]** | R1 = 0.0685, wR2 = 0.1778 | R1 = 0.0513, wR2 = 0.1209 | R1 = 0.0325, wR2 = 0.0822 |
| **R indices (all data)** | R1 = 0.1053, wR2 = 0.1993 | R1 = 0.0903, wR2 = 0.1395 | R1 = 0.0352, wR2 = 0.0834 |
| **Flack** | | | 0.3(16) * |

*inversion twin

# Crystal structures of cocrystals

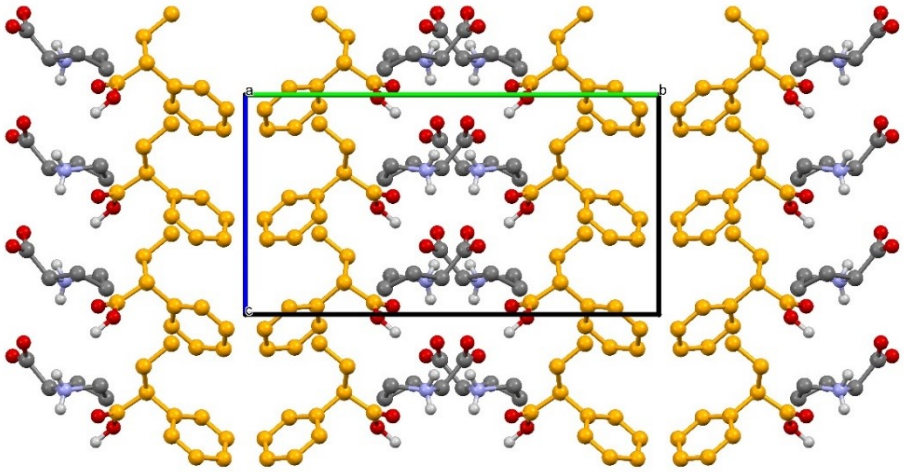


**Figure ESI-1**. Crystal structure of 2-PBA·PRO. View down crystallographic a-axis. $H_{CH}$ omitted and carbons of 2-phenylbutyric acid are orange for clarity.

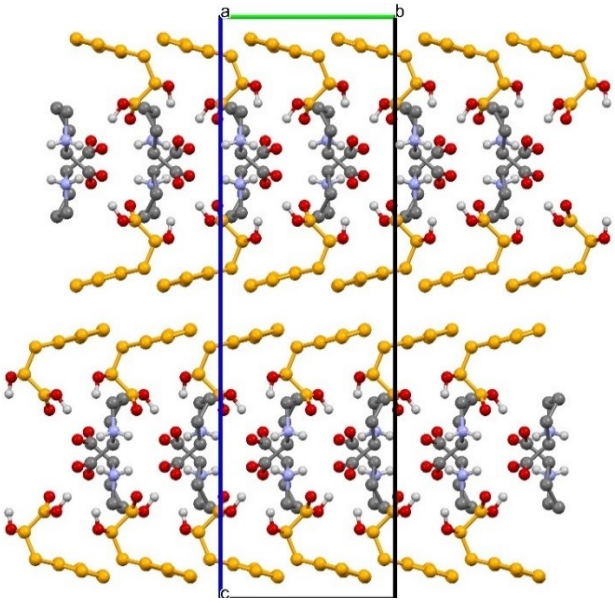


**Figure ESI-2**. Crystal structure of 3-PLA·PRO. View down crystallographic a-axis. $H_{CH}$ omitted and carbons of 3-phenyllactic acid are orange for clarity.

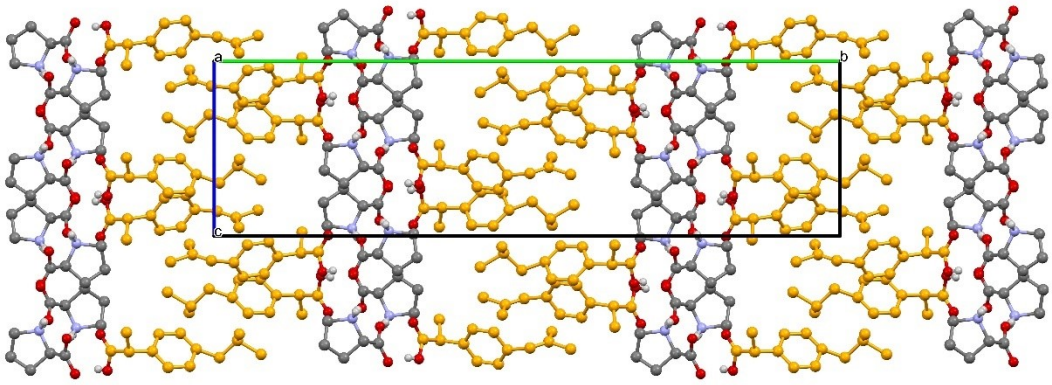


**Figure ESI-3**. Crystal structure of IBU·PRO. View down crystallographic a-axis. $H_{CH}$ omitted and carbons of ibuprofen are orange for clarity.

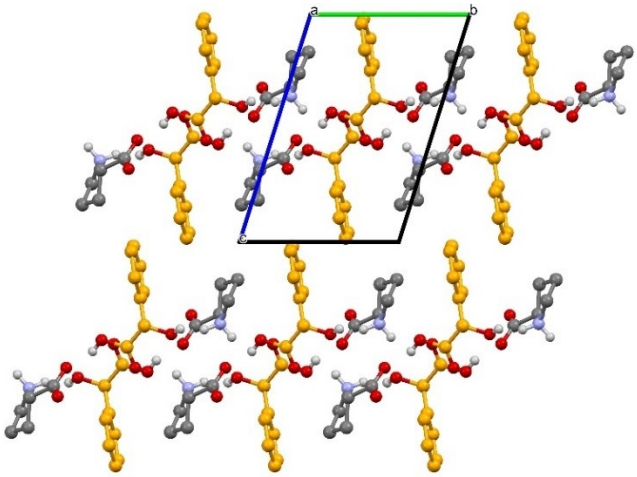


**Figure ESI-4**. Crystal structure of MA·PRO. View down crystallographic a-axis. $H_{CH}$ omitted and carbons of mandelic acid are orange for clarity.

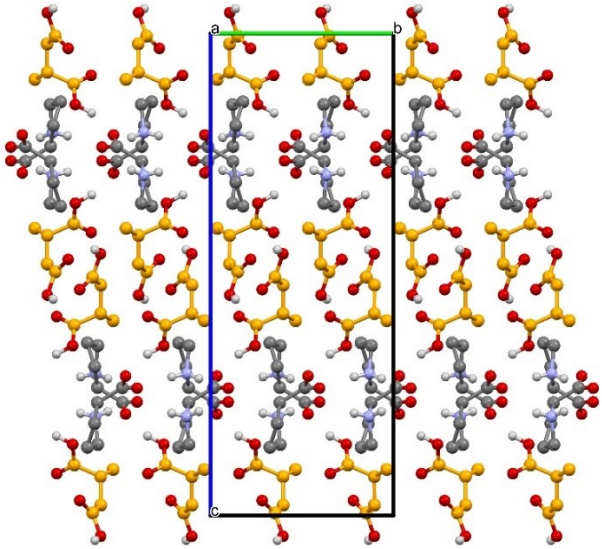


**Figure ESI-5**. Crystal structure of MSA·PRO. View down crystallographic a-axis. $H_{CH}$ omitted and carbons of methylsuccinic acid are orange for clarity.

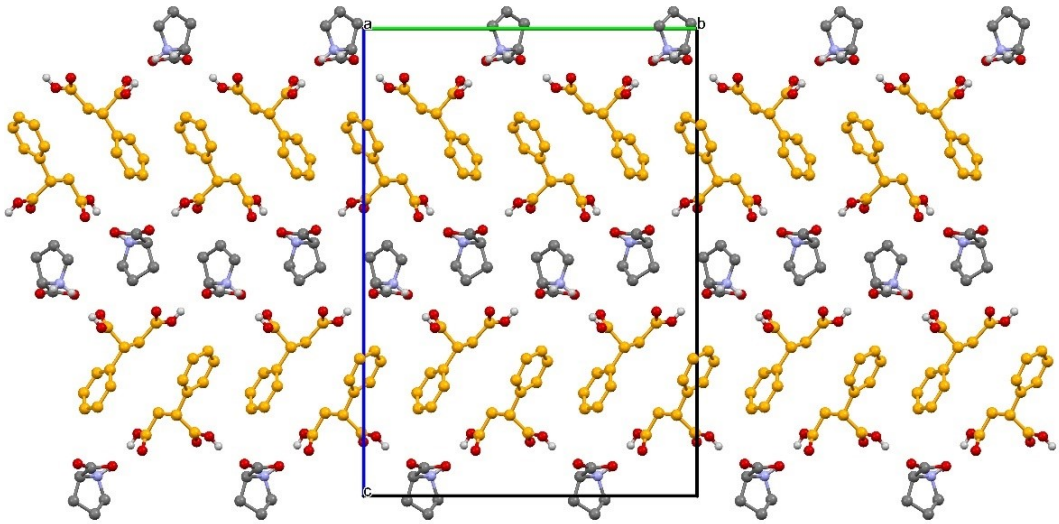


**Figure ESI-6**. Crystal structure of PSA·PRO. View down crystallographic a-axis. $H_{CH}$ omitted and carbons of phenylsuccinic acid are orange for clarity.

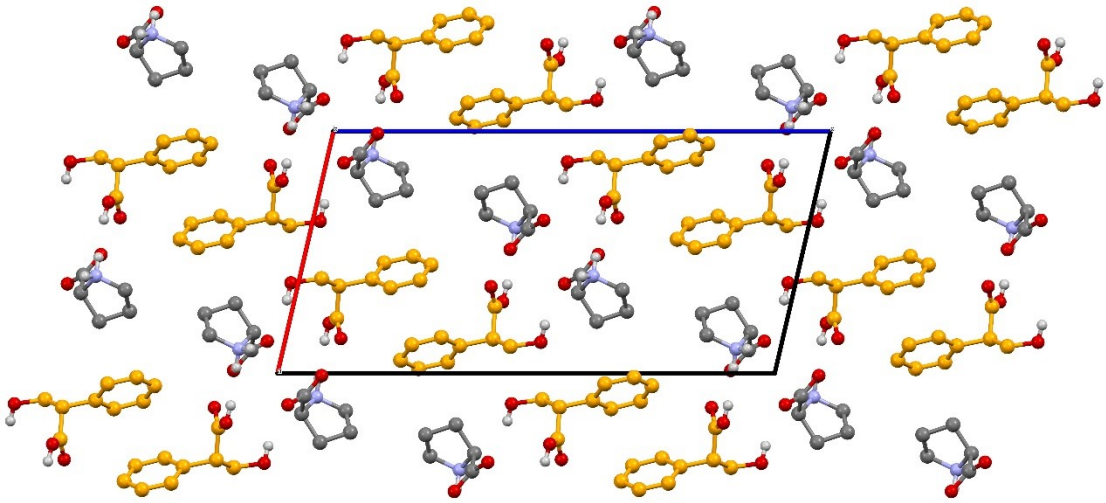

**Figure ESI-7**. Crystal structure of TRA·PRO. View down crystallographic b-axis. $H_{CH}$ omitted and carbons of tropic acid are orange for clarity.

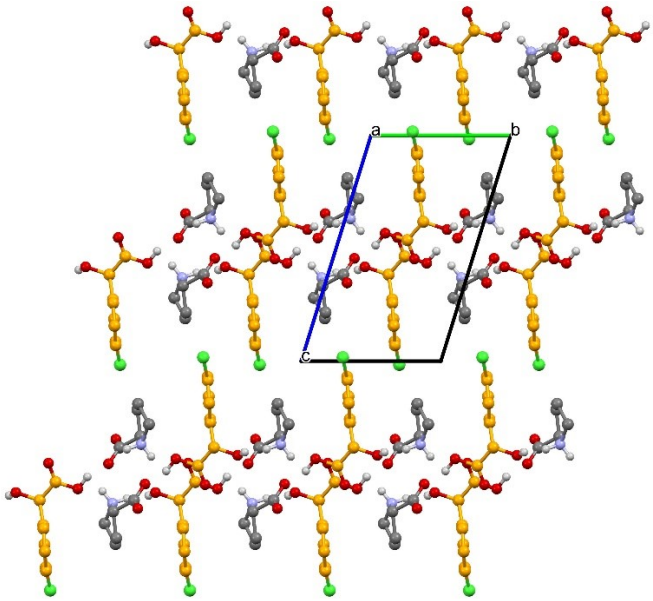


**Figure ESI-8**. Crystal structure of 3-CMA·PRO. View down crystallographic a-axis. $H_{CH}$ omitted and carbons of 3-chloromandelic acid are orange for clarity.

# Crystal structure of new polymorphs of the reagents

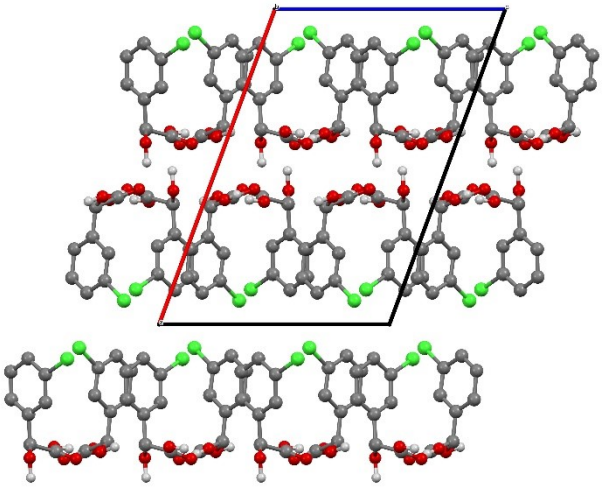

**Figure ESI-9**. Crystal structure of 3-CMA. View down crystallographic b-axis. $H_{CH}$ omitted for clarity.

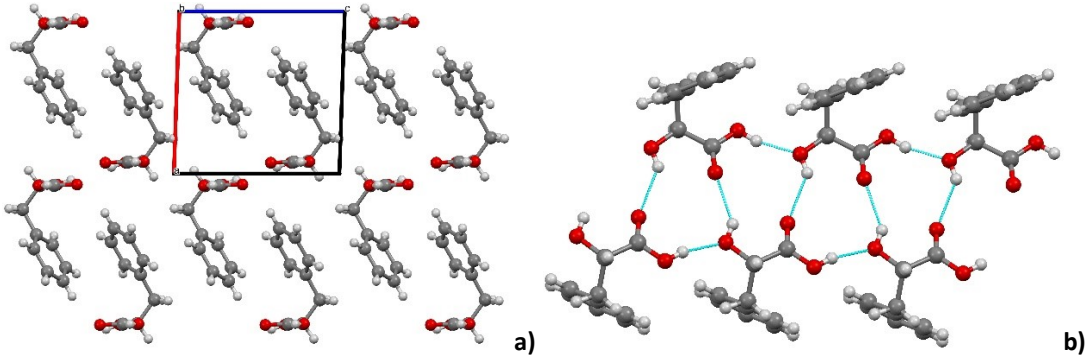


**Figure ESI-10**. S-3-Phenyllactic acid. (a) crystal packing, view down crystallographic b-axis; hydrogen bond interactions (b). $H_{CH}$ omitted for clarity.

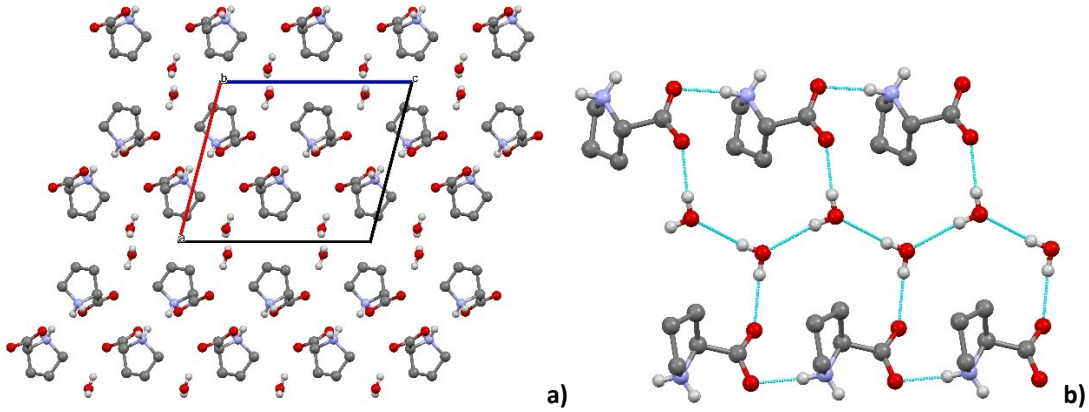


**Figure ESI-11**. DL-proline hydrate. (a) crystal packing, view down crystallographic b-axis; hydrogen bond interactions (b). $H_{CH}$ omitted for clarity.

# 1. The comparison of experimental and simulated XRPD patterns of the obtained cocrystals.

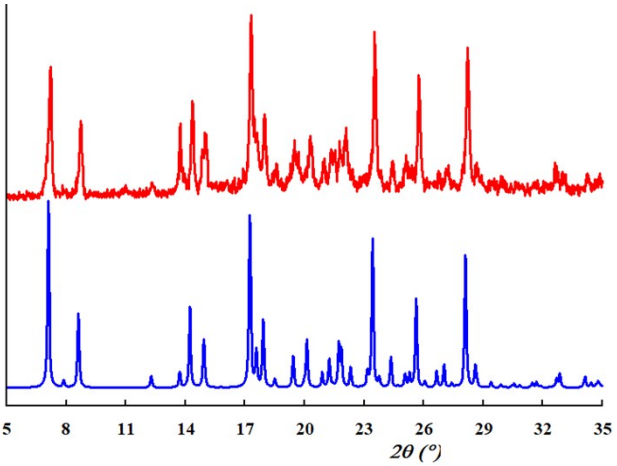


**Figure ESI-12**. Comparison of the experimental XRPD pattern of the grinding experiment between racemic etiracetam and mandelic acid (red) with the simulated one of S-MAN·S-ETI (refcode YAGSIK[1]).

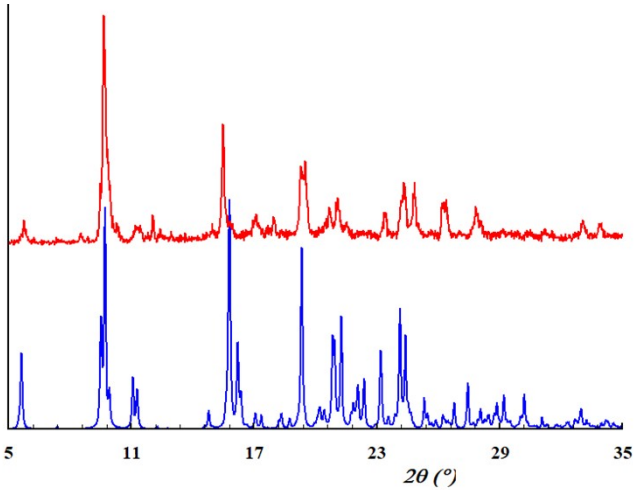


**Figure ESI-13**. FLU·ETI. Comparison of the experimental (red) and simulated (blue) XRPD patterns. Some traces of unreacted starting materials are present in the experimental pattern.

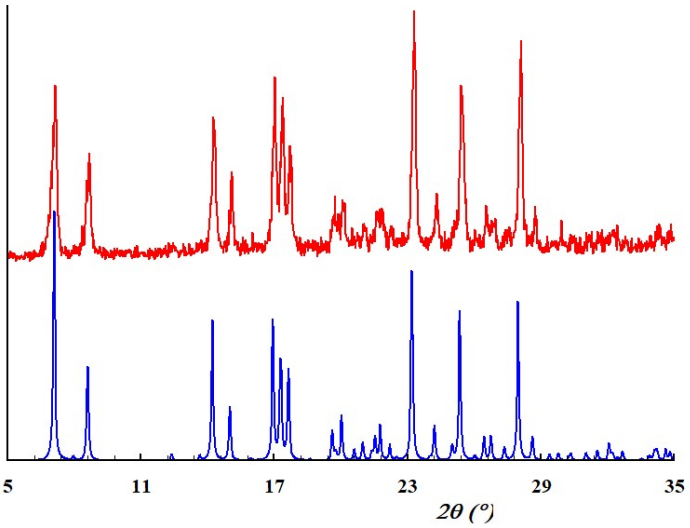


**Figure ESI-14**. 2-FMA·PRO. Comparison of the experimental (red) and simulated (blue) XRPD patterns.

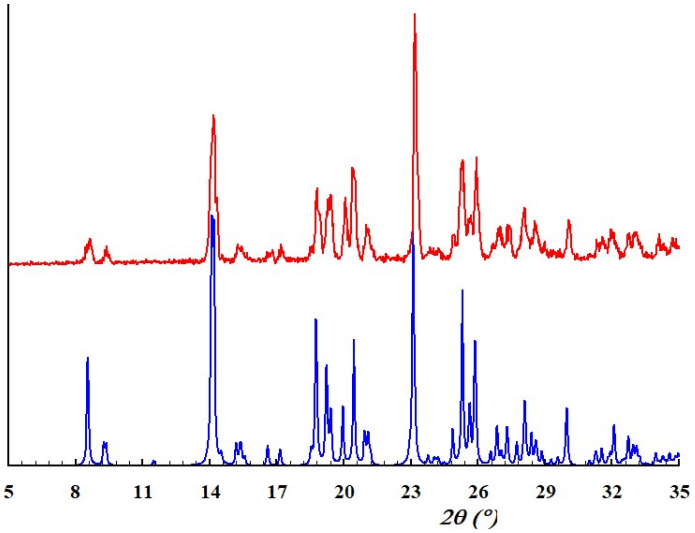


**Figure ESI-15**. 3-CMA·ETI. Comparison of the experimental (red) and simulated (blue) XRPD patterns.

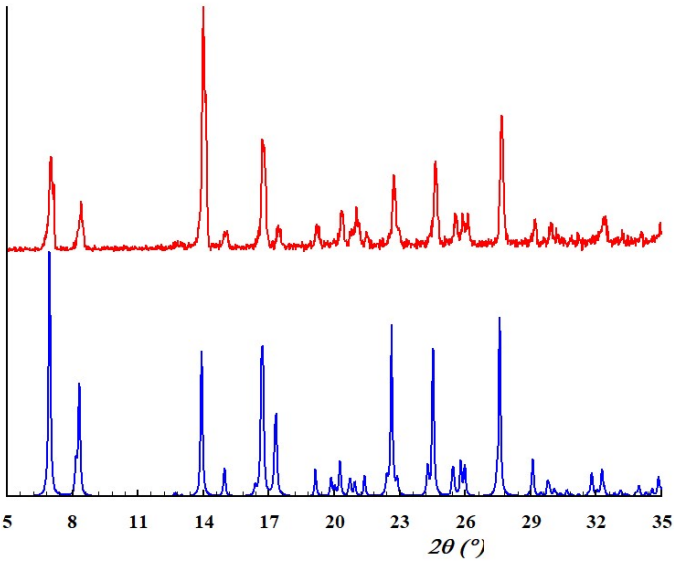


**Figure ESI-16**. 2-CMA·ETI. Comparison of the experimental (red) and simulated (blue) XRPD patterns.

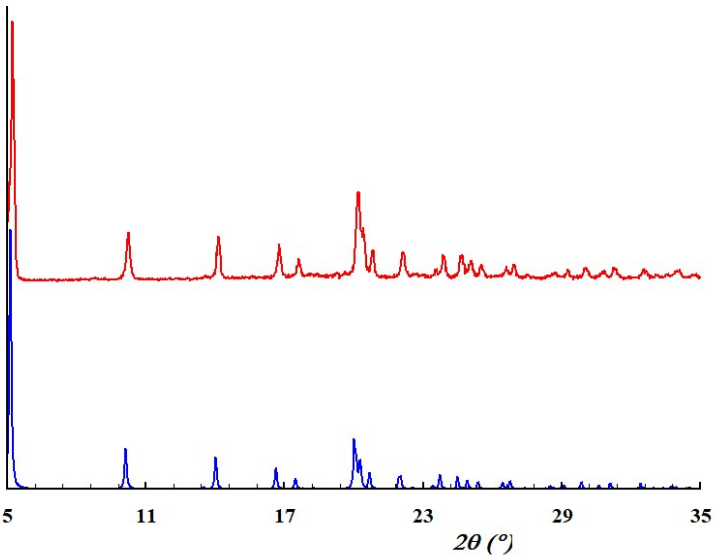


**Figure ESI-17**. PBA·PRO. Comparison of the experimental (red) and simulated (blue) XRPD patterns.

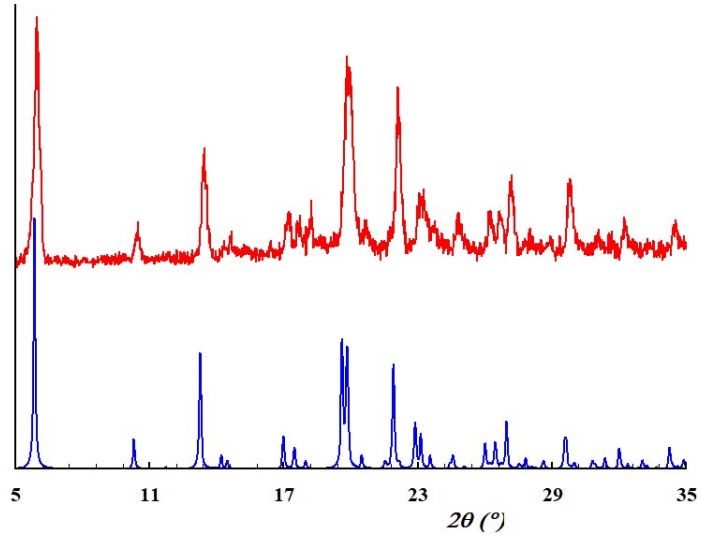


**Figure ESI-18**. 3-PLA·PRO. Comparison of the experimental (red) and simulated (blue) XRPD patterns.

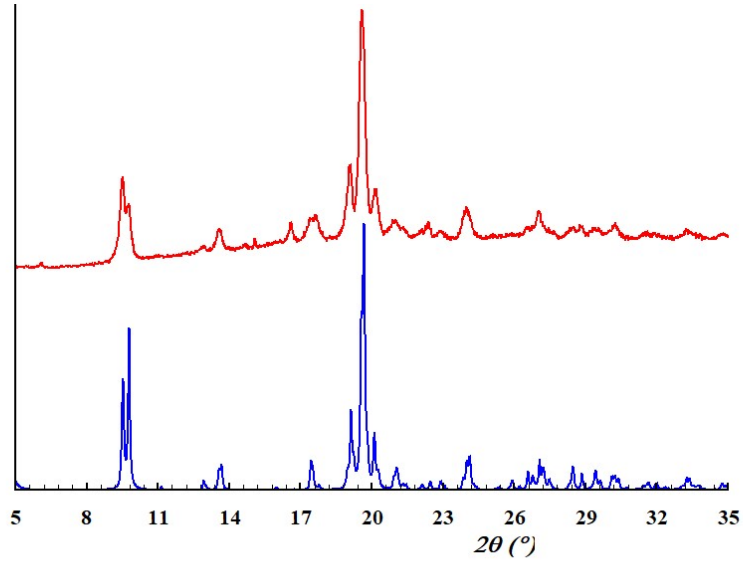


**Figure ESI-19**. IBU·PRO. Comparison of the experimental (red) and simulated (blue) XRPD patterns. Some traces of starting materials are present.

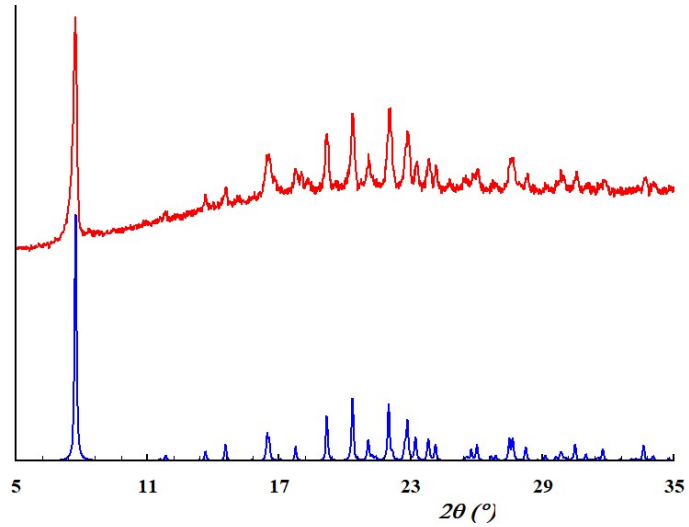


**Figure ESI-20**. MA·PRO. Comparison of the experimental (red) and simulated (blue) XRPD patterns.

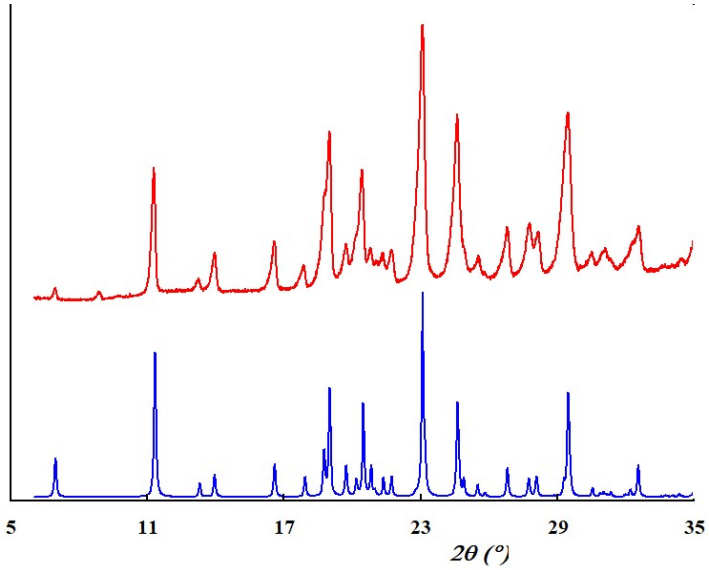


**Figure ESI-21**. MSA·PRO. Comparison of the experimental (red) and simulated (blue) XRPD patterns.

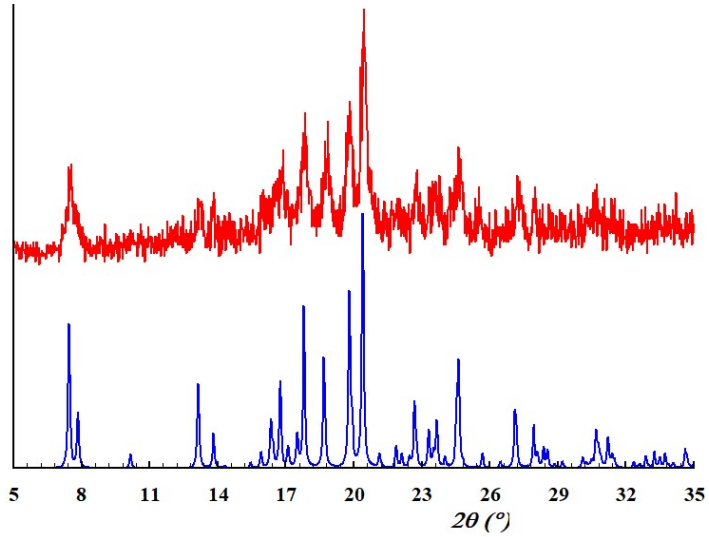


**Figure ESI-22**. FLU·PRO. Comparison of the experimental (red) and simulated (refcode VEVNOC,[2] blue) XRPD patterns.

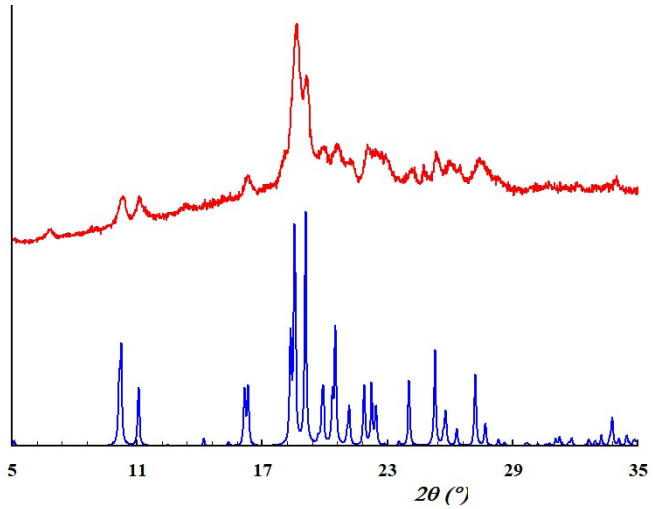


**Figure ESI-23**. NAP·PRO. Comparison of the experimental (red) and simulated (refcode QIMBEW,[3] blue) XRPD patterns. Some traces of unreacted starting materials are present.

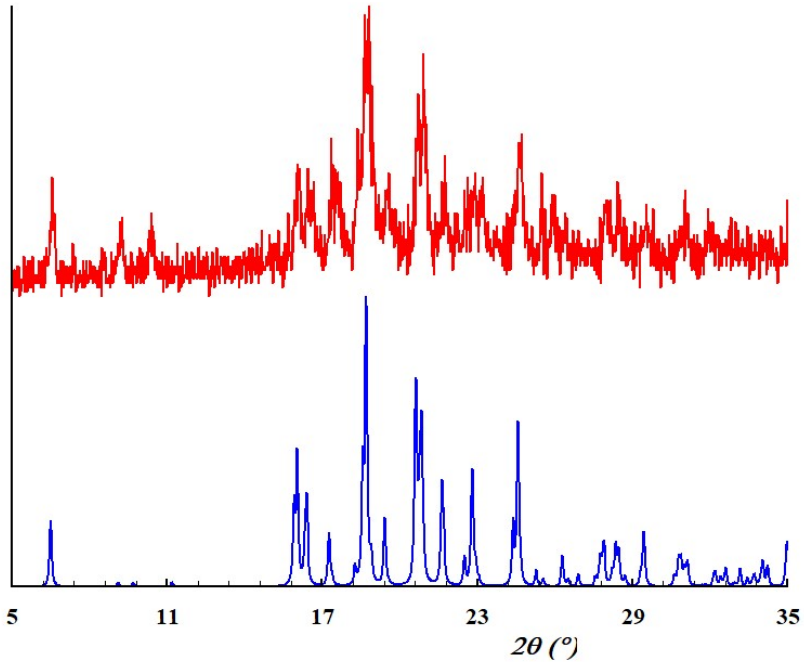


**Figure ESI-24**. PSA·PRO. Comparison of the experimental (red) and simulated (blue) XRPD patterns. Some traces of starting materials are present.

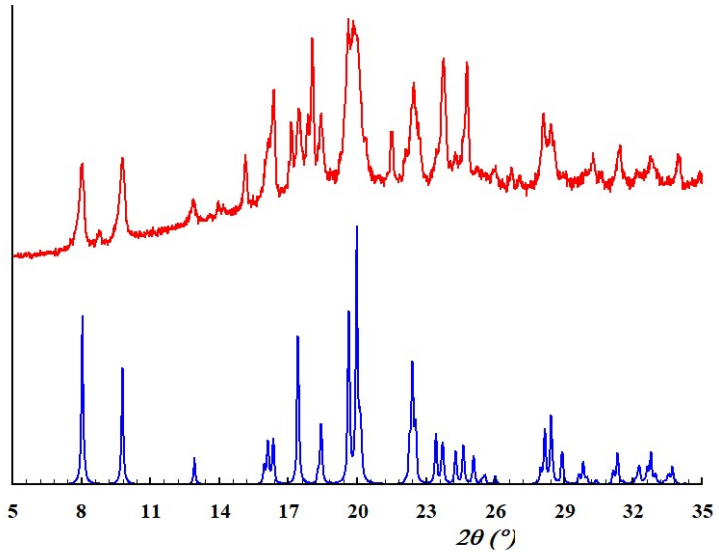


**Figure ESI-25**. TRA·PRO. Comparison of the experimental (red) and simulated (blue) XRPD patterns. Some traces of unreacted starting materials are present.

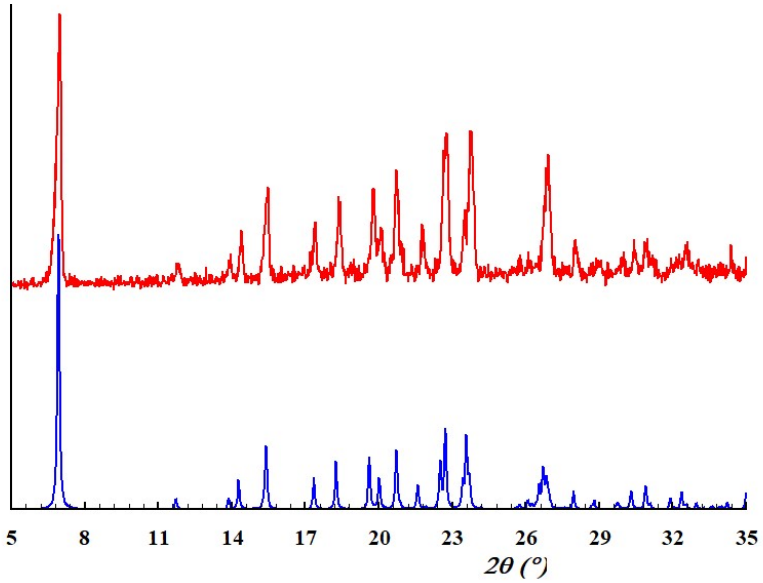


**Figure ESI-26**. 3-CMA·PRO. Comparison of the experimental (red) and simulated (blue) XRPD patterns.

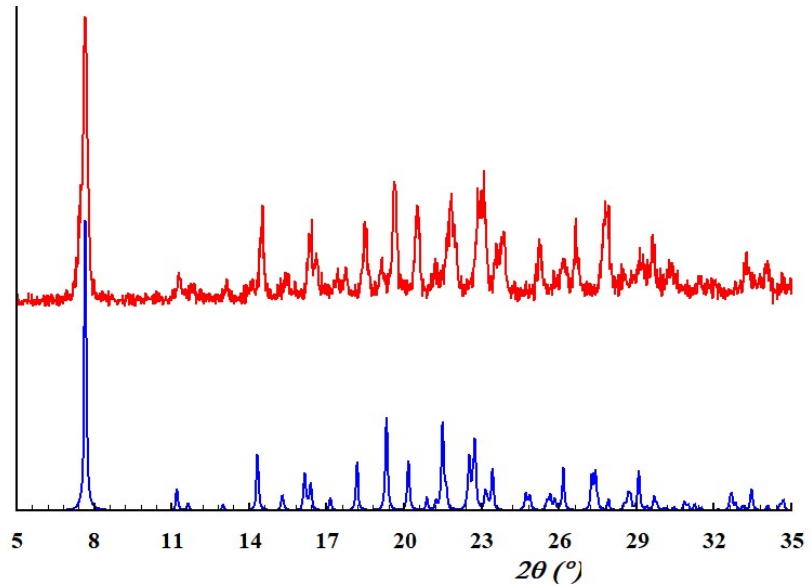


**Figure ESI-27**. 2-FMA·PRO. Comparison of the experimental (red) and simulated (blue) XRPD patterns.